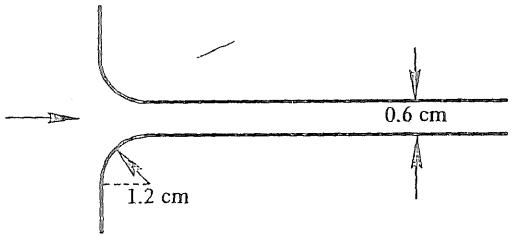


Figure 9-6

9-15 Water at 10°C flows from a reservoir through the convergent nozzle shown in Fig. 9-6 into a circular tube. The mass flow rate of the water is 9 g/s. Making a plausible assumption as to the origin of the boundary layer in the nozzle and assuming that the nozzle surface is at a uniform temperature different from 10°C, calculate the heat-transfer coefficient at the throat of the nozzle. How does this compare with the coefficient far downstream in the tube if the tube surface is at a uniform temperature?

## REFERENCES


1. Eckert, E. R. G.: *VDI-Forschungsh.*, vol. 416, 1942, pp. 1–24.
2. Schlichting, H.: *Boundary Layer Theory*, 6th ed., McGraw-Hill, New York, 1968.
3. Reshotko, E., and C. B. Cohen: NACA TN 3513 (now NASA), Washington, July 1955.
4. Mickley, H. S., R. C. Ross, A. L. Squyers, and W. E. Stewart: NASA TN 3208, Washington, 1954.
5. Emmons, H. W., and D. Leigh: Combustion Aerodynamics Laboratory Rept. 9, Harvard University, Cambridge, Mass., 1953.
6. Brown, W. B., and P. L. Donoughe: NASA TN 2489, Washington, 1951.
7. Donoughe, P. L., and J. N. B. Livingood: NASA TN 3151, Washington, 1954.
8. Livingood, J. N. B., and P. L. Donoughe: NASA TN 3588, Washington, 1955.
9. Howe, J. T., and W. A. Mersman: NASA TN D-12, Washington, D.C., 1959.
10. Dewey, C. F., Jr., and J. F. Gross: In *Advances in Heat Transfer*, vol. 4, Academic, New York, 1967, pp. 317–446.
11. Sparrow, E. M., and H. S. Yu, *J. Heat Transfer*, vol. 93, 1971, pp. 328–334.
12. Eckert, E. R. G., and R. M. Drake, Jr.: *Heat and Mass Transfer*, McGraw-Hill, New York, 1959, pp. 173–176.
13. Klein, J., and M. Tribus: ASME Paper 53-SA-46, ASME semiannual meeting, 1953.
14. Blottner, F. G.: In AGARD-LS-73 (NTIS AD-A013 269), von Kàrmàn Institute, Brussels, Belgium, February 1975.
15. Smith, A. G., and D. B. Spalding: *J. Roy. Aero. Soc.*, 62, vol. 62, 1958, p. 60.
16. Spalding, D. B.: *J. Fluid Mech.*, vol. 4, pt. 1, May 1958, p. 22.
17. Brown, S. N., and K. Stewartson: In *Annual Review of Fluid Mechanics*, vol. 1, 1969, pp. 45–72.
18. Williams, J. C., III: In *Annual Review of Fluid Mechanics*, vol. 9, 1977, pp. 113–144.
19. Morgan, V. T.: In *Advances in Heat Transfer*, vol. 11, Academic, New York, 1975, pp. 199–264.
20. Raithby, G. D., and E. R. G. Eckert: *Int. J. Heat Mass Transfer*, vol. 11, 1968, pp. 1133–1152.
21. Kays, W. M., and A. L. London: *Compact Heat Exchangers*, 2d ed., McGraw-Hill, New York, 1964.
22. Zukauskas, A.: In *Advances in Heat Transfer*, vol. 8, 1972, pp. 93–160.


CHAPTER

# TEN

# MOMENTUM TRANSFER: THE TURBULENT MOMENTUM BOUNDARY LAYER

In this chapter the stability of the laminar boundary layer is discussed, and a transition to a turbulent type of boundary layer is described. The characteristics of the turbulent boundary layer are discussed in general terms, and then the Prandtl mixing-length theory is introduced as a method of solving the turbulent boundary-layer equations. This leads to the concept of a viscous sublayer and the development of the "law of the wall." Then approximate algebraic solutions to the momentum boundary layer are developed, as well as more precise procedures that require computer implementation. Throughout the chapter all fluid properties are treated as constant.

It is impossible to acknowledge and/or reference all the researchers who have contributed to the present state of knowledge of turbulent flows. However, there do exist treatises which, with their combined bibliographies, describe the bulk of the research contributions through the late 1970s. These include Bradshaw,[1] Launder and Spalding,[2] Hinze,[3] Rotta,[4] Tennekes and Lumley,[5] and Townsend,[6] all of which are recommended to the reader for further study.

## TRANSITION OF A LAMINAR BOUNDARY LAYER TO A TURBULENT BOUNDARY LAYER

An important characteristic of a laminar boundary layer, and of a laminar flow in a pipe or duct, is that under certain conditions the flow is unstable in the presence of small disturbances, and a transition to a fundamentally

different kind of flow, a turbulent flow, can occur. The viscous forces, largely responsible for the characteristics of a laminar flow, have the effect of restoring a laminar flow to its previous state when it is subjected to an external disturbance; on the other hand, inertia forces associated with local transient velocity changes have quite the opposite effect. Inertia forces tend to be destabilizing and thus to amplify local disturbances. The Reynolds number is a ratio of inertia to viscous forces, and thus one might well expect that the stability of a laminar flow is in considerable part associated with the value of the Reynolds number, stable laminar flows being associated with low values of the Reynolds number.

For a simple laminar boundary layer on a flat, smooth surface with no pressure gradient, it is found in typical laboratory wind tunnel experiments that a transition to a turbulent type of boundary layer tends to occur when the length Reynolds number $\mathrm{Re}_x$ reaches the range 300,000 to 500,000. But this particular range of critical Reynolds numbers seems to be associated with the surface roughness and free-stream disturbances characteristic of typical laboratory wind tunnels for low-speed flows. Laminar boundary layers have been observed to persist to Reynolds numbers several orders of magnitude higher if the free stream has no pressure fluctuations and the surface is very smooth. Such conditions frequently occur during the reentry of space vehicles into the earth's atmosphere.

At the low Reynolds numbers it is found experimentally that a laminar boundary layer under zero pressure gradient is stable to even very large disturbances when the length Reynolds number is less than about 60,000. Similarly, it is found that fully developed laminar flow in a pipe or duct is stable to large disturbances if the Reynolds number based on hydraulic diameter is less than about 2300.

There exists a theory of *viscous stability*, for that is what we are discussing here, and for small disturbances (which permit a linearized theory) it is found that the laminar external boundary layer for zero pressure gradient is stable for $\mathrm{Re}_x$ less than about 60,000. A review of viscous stability theory leading to this value is given by Shen.[7] It can also be shown that a "favorable" pressure gradient, an accelerating flow, leads to higher critical Reynolds numbers, and an "unfavorable" pressure gradient, or decelerating flow, leads to lower critical Reynolds numbers. Suction or blowing at the surface might be expected to have similar effects. Reviews of boundary-layer stability and transition are given by Tani[8] for low-speed flows and by Reshotko[9] for high-speed flows.

The length Reynolds number $\mathrm{Re}_x$ is not a particularly convenient parameter to use for a transition criterion because it has useful significance only for flows of constant free-stream velocity and zero pressure gradient. If it is assumed that the phenomenon is primarily a local one, then a local Reynolds number criterion might be more generally useful. Either the displacement or momentum thickness Reynolds number might be used, but since the momentum thickness Reynolds number must generally be evaluated anyway in most applications, its use is suggested here.



Let us evaluate the momentum thickness Reynolds number $\mathrm{Re}_{\delta_2}$ for the laminar, zero-pressure-gradient boundary layer as it reaches its lower critical Reynolds number, $\mathrm{Re}_x = 60{,}000$.

From Eq. (7-20)

$$\delta_2 = 0.664\sqrt{\frac{\nu x}{u_\infty}}$$

Then

$$\mathrm{Re}_{x,\,\mathrm{crit}} = 60{,}000 = \frac{u_\infty x}{\nu}$$

Combine and eliminate $x$:

$$60{,}000 = \frac{(u_\infty \delta_2/\nu)^2}{0.442}$$

But

$$\frac{u_\infty \delta_2}{\nu} = \mathrm{Re}_{\delta_2}$$

Thus

$$\mathrm{Re}_{\delta_2,\,\mathrm{crit}} = 162 \tag{10-1}$$

This value of $\mathrm{Re}_{\delta_2}$ is now proposed as a general criterion for transition whenever substantial free-stream disturbances are present, regardless of pressure gradient or mass transfer at the surface, and this seems to correspond with the experimental facts. The laminar boundary layer can, of course, persist to higher values of $\mathrm{Re}_{\delta_2}$ under undisturbed conditions. A strongly accelerated laminar boundary layer may have a somewhat higher critical Reynolds number, but such an acceleration inhibits the growth of $\mathrm{Re}_{\delta_2}$ (it can actually decrease) so the point is usually moot.

It is interesting to note that if the equivalent of the momentum thickness Reynolds number is evaluated for fully developed laminar flow in a duct at a value of the hydraulic diameter Reynolds number equal to 2300, almost the same value of $\mathrm{Re}_{\delta_2}$ is found as for the simple external boundary layer. This further suggests the general applicability of Eq. (10-1).

## THE QUALITATIVE STRUCTURE OF THE TURBULENT BOUNDARY LAYER

The breakdown of the laminar boundary layer discussed in the preceding section does not occur everywhere across the flow at the same distance $x$. It occurs at certain favorable "spots" and then spreads laterally downstream

until the entire boundary layer is engulfed. Thus there is a three-dimensional aspect to transition, and there is a distinct "transition region" which can be as long as or longer than the purely laminar region. Ultimately a fully developed turbulent boundary layer is established, and this new boundary layer is again, on the average, two-dimensional to the same order as the preceding laminar boundary layer.

We are not going to attempt here to develop a theory for the "transition region," other than to suggest that in engineering design the extent of this region can be assumed to be about the same length as the laminar region, and that the friction, heat-transfer, and mass-transfer coefficients vary continuously from the laminar to the fully developed turbulent region. The reader should consult Ref. 10 for a summary of abstracts dealing in part with prediction models for transition. With this said, we are going to skip forward to the fully developed turbulent region. Let us first see what it looks like and what seems to be happening.

The important characteristics of a turbulent flow adjacent to a solid surface differ little whether we are speaking of a turbulent external boundary layer or fully developed turbulent flow in a pipe or duct. Experimentally at least two regions are observed: (1) a predominantly viscous region immediately adjacent to the wall surface where the momentum and heat transfer can be largely accounted for by the simple mechanisms of viscous shear and molecular conduction; and (2) a fully turbulent region, comprising most of the boundary layer, where velocity is nowhere independent of time, where "eddy" motion is observed, and where momentum and heat are transported at rates generally much greater than can be accounted for by viscous shear and molecular conduction.

Examination of the fully turbulent region reveals that the velocity at any point in space seems to consist of a relatively large *time-averaged velocity*, upon which is superimposed a small fluctuating velocity with instantaneous components in all directions. The existence of velocity components *normal* to the mean velocity vector means that fluid is moving, at least momentarily, in the normal direction; this fluid carries with it *momentum*—it may carry *thermal energy*, or any other property for which there is a mean gradient in the normal direction; and, in fact, this is the primary mechanism whereby such effects are transported in the normal direction.

Further examination of the fully turbulent region reveals that the velocity fluctuations are the result of *vorticity* in the fluid. In fact, virtually every particle is a part of fluid eddies that are turning over in various directions, and this is what we mean by a turbulent flow.

The thin, viscous region close to the wall, which we will call the *viscous sublayer*, is actually of more importance than the fully turbulent region. It is in this sublayer that events leading to the production of turbulence occur, events that are described by Offen and Kline[11] and summarized by Hinze.[12] A simple description of the sublayer is that it is essentially a continually developing laminar boundary layer which grows until its local Reynolds number becomes supercritical, at which point it becomes locally unstable and suffers a local breakdown. The breakdown is identified with a "burst" of turbulence from the wall region. The bursts are sufficiently frequent in both space and time to cause the sublayer to maintain, on the average, a constant thickness Reynolds number.

A "burst" resulting from local instability is a three-dimensional event that results in the *ejection* from the wall region of a relatively large element of slow-moving fluid, which moves out into the fully turbulent region, and its replacement by a similar element of higher-velocity fluid. Although there is some momentum (and heat) transfer within the sublayer associated with these events, viscous shear (and molecular conduction) remains the predominant transport mechanism within the sublayer, especially very close to the wall, because of the relative infrequency of the event. But these elements colliding with the higher-velocity fluid in the fully turbulent region outside the sublayer provide the primary source of the *turbulent mechanical energy* in that region, i.e., the kinetic energy of the eddies. While turbulent kinetic energy is being generated by the collision of finite higher-velocity elements of fluid with low-velocity fluid, the viscosity of the fluid is acting to decay the eddies and transform the turbulent energy into thermal energy. A new *state of stability* is established in which the production of turbulent energy is equal to the dissipation of that energy plus a certain part which is convected and diffused outward.

In a sense, then, the turbulent boundary layer is a *stable region* possessing the property of *diffusing momentum*, and other properties, very much more rapidly than by simple molecular processes. Although an *instability* in the sublayer is an essential feature, the overall structure is completely stable, self-adjusting, and repeatable.

As we move along the surface, the turbulent boundary layer grows, like the laminar boundary layer, and its momentum thickness Reynolds number grows. But the sublayer maintains essentially the same thickness Reynolds number and thus becomes a smaller and smaller fraction of the overall boundary layer.

## THE CONCEPT OF EDDY DIFFUSIVITY, EDDY VISCOSITY

A useful, though not totally necessary, concept is now introduced. To make turbulent boundary-layer calculations, we need either information or a theory to evaluate the term $\overline{u'v'}$ in Eq. (4-46). This is frequently referred to in the literature as the turbulence "closure" problem, and it is usually solved by solving an algebraic equation, or a differential equation, for $\overline{u'v'}$. In Chap. 4 $\overline{u'v'}$ is defined as an apparent *turbulent stress*, and it seems plausible

that it goes to zero if there is no gradient in the mean velocity profile. In actual fact, this is not precisely so, but it is close enough for many practical applications. Thus it seems reasonable to state that

$$\overline{u'v'} \propto \frac{\partial \bar{u}}{\partial y}$$

As a proportionality factor we define the *eddy diffusivity for momentum* $\varepsilon_M$,

$$\overline{u'v'} = -\varepsilon_M \frac{\partial \bar{u}}{\partial y} \tag{10-2}$$

This is nothing but a definition; we still have the problem of evaluating $\varepsilon_M$.

Let us now examine some of the implications of this definition. When (10-2) is substituted into Eq. (4-46), the momentum differential equation for the simple, constant-property, turbulent boundary layer becomes

$$\bar{u}\frac{\partial \bar{u}}{\partial x} + \bar{v}\frac{\partial \bar{u}}{\partial y} - \frac{\partial}{\partial y}\left[(\nu + \varepsilon_M)\frac{\partial \bar{u}}{\partial y}\right] + \frac{1}{\rho}\frac{d\bar{P}}{dx} = 0 \tag{10-3}$$

$\varepsilon_M$ is dimensionally the same as $\nu$, and the turbulent contribution to diffusion in the $y$ direction thus can be readily compared to the molecular contribution. In most cases it is found that $\varepsilon_M \gg \nu$ in the fully turbulent region, while $\nu \gg \varepsilon_M$ in the viscous sublayer close to the wall.

It is sometimes convenient to define an *eddy viscosity* $\mu_t$. By simple analogy with the corresponding molecular quantities,

$$\mu_t = \rho\varepsilon_M \tag{10-4}$$

## THE PRANDTL MIXING-LENGTH THEORY

The Prandtl mixing-length theory is merely one of several schemes which have been used to evaluate $\overline{u'v'}$ (or $\varepsilon_M$) in the calculation of turbulent boundary-layer flows. The theory of turbulent wall shear layers is presently in a state of intense study, and new breakthroughs are continually in sight. But the simplest of all the schemes proposed remains the very old Prandtl mixing-length theory; and with new information available on the very important behavior of the viscous sublayer, the mixing-length theory provides a remarkably adequate basis for many engineering applications. We rely on it entirely in this book.

The defining equation for the mixing length can be very simply stated as a starting hypothesis. The development following is provided not as a *proof* of anything, but rather as a plausible argument for the *form* of the mixing-length equation. Later in Chap. 12 in connection with the Reynolds analogy we discuss a more physical argument for the same equation.



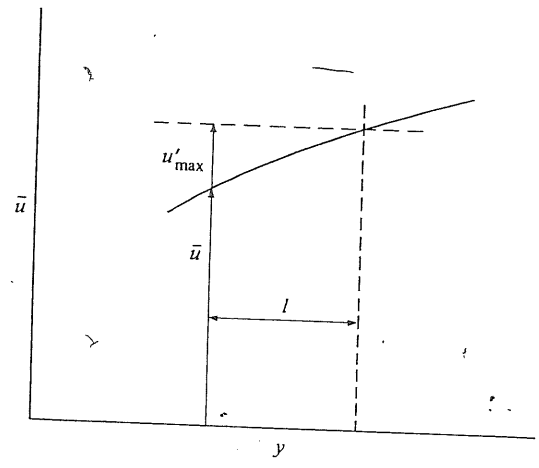


**Figure 10-1** Graphical definition of the mixing length.

Let us idealize the turbulent fluctuating-velocity components $u'$ and $v'$ as simple harmonic functions having the same period $\theta_1$ but differing amplitudes and phase angles. That is,

$$u' = u'_{max} \sin \frac{2\pi\theta}{\theta_1}$$

$$v' = v'_{max} \sin \frac{2\pi(\theta + \alpha_1)}{\theta_1}$$

Next, form the time average of the product of $u'$ and $v'$:

$$\overline{u'v'} = \frac{1}{\theta_1}\int_0^{\theta_1} u'v'\, d\theta = \frac{u'_{max}v'_{max}}{2}\cos\frac{2\pi\alpha_1}{\theta_1}$$

From this result we see that if $u'$ and $v'$ are in phase, or nearly in phase, the "turbulent shear stress" $\overline{u'v'}$ is a finite quantity, although it is also possible for $\overline{u'v'}$ to be zero (if $\alpha_1/\theta_1 = \frac{1}{4}$). The first condition apparently does obtain when there is a *gradient* in the mean velocity profile because we do observe substantial turbulent shear stresses in such situations.

Now let us define a "mixing length" $l$ in the manner illustrated in Fig. 10-1. If $l$ is small relative to the other dimensions of the system, then, approximately,

$$u'_{max} = l\left|\frac{\partial \bar{u}}{\partial y}\right|$$

Next let us assume that

$$v'_{max} = ku'_{max} = kl\left|\frac{\partial \bar{u}}{\partial y}\right|$$

where $k$ is simply a local constant. Then, for the case of $\alpha_1 = 0$ we obtain

$$\overline{u'v'} = \frac{u'_{\max} v'_{\max}}{2} = \frac{k}{2} l^2 \left(\frac{\partial \bar{u}}{\partial y}\right)^2$$

Next, absorb $k$ and $-\frac{1}{2}$ into $l$, which has as yet to be determined anyway, and we obtain the defining equation for the mixing length:

$$\overline{u'v'} = -l^2 \left(\frac{\partial \bar{u}}{\partial y}\right)^2 \tag{10-5}$$

If we prefer to express the mixing length $l$ in terms of $\varepsilon_M$ and/or $\mu_t$, we can then use Eqs. (10-2) and (10-4) to obtain

$$\varepsilon_M = l^2 \left|\frac{\partial \bar{u}}{\partial y}\right| \qquad \mu_t = \rho l^2 \left|\frac{\partial \bar{u}}{\partial y}\right| \tag{10-6}$$

We are still faced with the proposition of assigning a value to $l$, but here simple dimensional reasoning can be useful. Prandtl reasoned that in the region not too distant from the wall the only significant length dimension is distance from the wall, and thus it is reasonable to assume that $l$ scales on that distance. If we let the proportionality factor be $\kappa$, we then obtain

$$l = \kappa y \tag{10-7}$$

The validity of all these assumptions rests on whether $\kappa$ does, in fact, turn out to be a constant when measured at various points in the boundary layer. Figure 10-2 shows some typical experimental measurements of $l$ at five

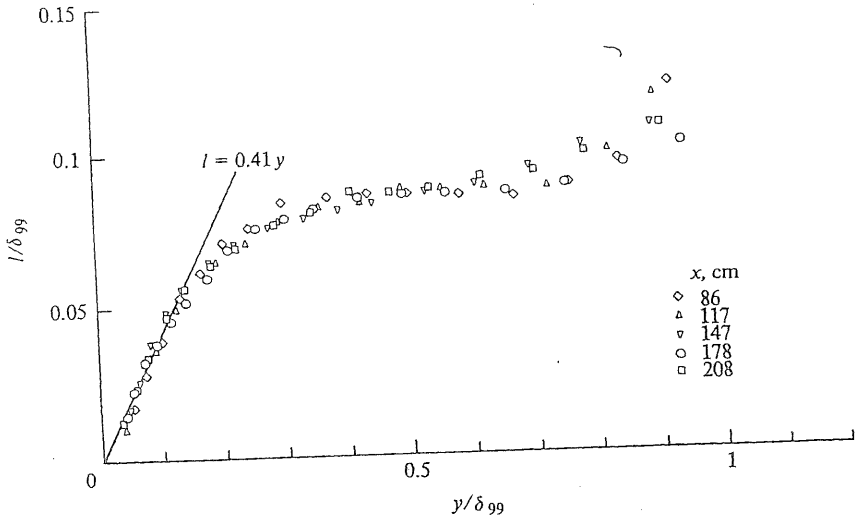


Figure 10-2 Mixing-length measurements of Anderson et al.[13] for an equilibrium weak adverse pressure gradient boundary layer.

different stations along a surface ($\delta_{99}$ is the boundary-layer thickness at the point where $\bar{u}/u_\infty = 0.99$). In the region near the wall, the data do indeed appear to be well represented by Eq. (10-7) with $\kappa$ taking on a value of about 0.41 ($\kappa$ is usually called the von Kármán constant).

There remains a region still closer to the wall, the viscous sublayer, where Eq. (10-7) is no longer valid, but the measurements shown on Fig. 10-2 do not go in this close. We discuss this region later. In the outer part of the boundary layer, on the other hand, it is apparent from Fig. 10-2 that the mixing length is proportional to total boundary-layer thickness rather than to distance from the wall; and since the value of $l$ becomes relatively unimportant for $y/\delta_{99}$ greater than about 0.7, the outer region can be quite adequately approximated by

$$l = \lambda \delta_{99} \tag{10-8}$$

where $\lambda$ is typically about 0.085.

The same behavior is noted for adverse pressure gradients, favorable pressure gradients, blowing, and suction, and the observed values of $\kappa$ and $\lambda$ seem little affected by these differing boundary conditions. Strictly speaking, these observations are valid only for so-called *equilibrium* boundary layers, a subject that is discussed later, but the turbulent boundary layer tends to approach *equilibrium* remarkably quickly.

## THE SHEAR-STRESS DISTRIBUTION NEAR A WALL

We still have not discussed the viscous sublayer, but that can be more conveniently done in terms of a new coordinate system which will be introduced shortly. First we develop an expression for the distribution of the total shear stress near the wall.

From the definition of $\varepsilon_M$ and the viscosity coefficient, the *total* apparent shear stress, molecular plus turbulent, can be expressed as

$$\frac{\tau}{\rho} = (\nu + \varepsilon_M)\frac{\partial \bar{u}}{\partial y} \tag{10-9}$$

Substituting (10-9) into Eq. (10-3), we obtain

$$\rho \bar{u}\frac{\partial \bar{u}}{\partial x} + \rho \bar{v}\frac{\partial \bar{u}}{\partial y} - \frac{\partial \tau}{\partial y} + \frac{d\bar{P}}{dx} = 0 \tag{10-10}$$

[Note that Eq. (10-10) does not include any assumption about the shear mechanism; in fact, it is also valid for a steady laminar boundary layer.]

Let us now confine our attention to a region relatively close to the wall such that $\rho\bar{u}(\partial\bar{u}/\partial x)$ is enough smaller than the other terms that it can be neglected. We are talking about a region that generally extends outside the viscous sublayer and in some cases can include as much as one-third of the

entire boundary layer. We call this a *Couette flow* assumption and speak of a *Couette flow region.*

Under this assumption $\bar{u} = \bar{u}(y)$ alone, Eq. (10-10) becomes an ordinary differential equation, and $\bar{v} = v_0$, the value of the normal velocity component at the wall surface.

$$\rho v_0 \frac{d\bar{u}}{dy} - \frac{d\bar{\tau}}{dy} + \frac{d\bar{P}}{dx} = 0 \tag{10-11}$$

Equation (10-11) can now be integrated with respect to $y$ between the limits $\tau = \tau_0$ and $\bar{u} = 0.0$, at $y = 0$ and corresponding values at any distance $y$:

$$\frac{\tau}{\tau_0} = 1 + \frac{\rho v_0 \bar{u}}{\tau_0} + \left(\frac{d\bar{P}}{dx}\right)\frac{y}{\tau_0} \tag{10-12}$$

Next we introduce some nondimensional variables that are used extensively in turbulent boundary-layer analysis and are sometimes referred to as *wall coordinates*. First, from the definition of the friction coefficient we define a *shear velocity*, or *friction velocity*, $u_\tau$:

$$\frac{\tau_0}{\rho} = \frac{c_f u_\infty^2}{2} = u_\tau^2$$

Thus

$$u_\tau = \sqrt{\tau_0/\rho}$$

Note that $u_\tau$ has the dimension of velocity. (It is sometimes given the symbol $u_*$ in the literature.) Next the following dimensionless groups can be formed:

$$u^+ = \frac{\bar{u}}{u_\tau} = \frac{\bar{u}}{\sqrt{\tau_0/\rho}} = \frac{\bar{u}/u_\infty}{\sqrt{c_f/2}}$$

$$y^+ = \frac{yu_\tau}{\nu} = \frac{y\sqrt{\tau_0/\rho}}{\nu} = \frac{yu_\infty\sqrt{c_f/2}}{\nu}$$

$$v_0^+ = \frac{v_0}{u_\tau} = \frac{v_0}{\sqrt{\tau_0/\rho}} = \frac{v_0/u_\infty}{\sqrt{c_f/2}}$$

$$p^+ = \frac{\mu(d\bar{P}/dx)}{(\rho^{1/2}\tau_0^{3/2})}$$

When these are substituted into Eq. (10-12), we obtain

$$\frac{\tau}{\tau_0} = 1 + v_0^+ u^+ + p^+ y^+ \tag{10-13}$$

Note that Eq. (10-13) is valid only in the region where the Couette flow assumption is valid; at the outer edge of the boundary layer $\tau/\tau_0$ must go to zero.



## THE LAW OF THE WALL FOR THE CASE OF $p^+ = 0.0$ AND $v_0^+ = 0.0$

For this elementary case, in the Couette flow region Eq. (10-13) reduces to

$$\frac{\tau}{\tau_0} = 1.0$$

To obtain the law of the wall, we integrate Eq. (10-9) under this condition. Thus,

$$\frac{\tau_0}{\rho} = (\nu + \varepsilon_M)\frac{d\bar{u}}{dy} \tag{10-14}$$

Now we propose a model of the turbulent boundary layer which will consist of two very distinct regions, a *viscous sublayer* for which we assume $\nu \gg \varepsilon_M$ and a fully *turbulent region* for which $\varepsilon_M \gg \nu$. Later we examine a somewhat better model.

For the *viscous sublayer*, Eq. (10-14) reduces to

$$d\bar{u} = \frac{\tau_0}{\rho\nu}\,dy = \frac{\tau_0}{\mu}\,dy$$

Integrating from the wall,

$$\int_0^{\bar{u}} d\bar{u} = \frac{\tau_0}{\mu}\int_0^y dy$$

$$\bar{u} = \frac{\tau_0}{\mu}y$$

Now introduce the definitions of $u^+$ and $y^+$, and we obtain

$$u^+ = y^+ \tag{10-15}$$

Next we face the question of the effective thickness of the sublayer. Experimentally we find that the sublayer thickness can be expressed in terms of a critical value of $y^+$, and this value remains unchanged regardless of the total thickness of the boundary layer. The *reason* is that $y^+$ is simply a thickness Reynolds number, and the stability of the viscous sublayer is such that this Reynolds number always remains a constant at the outer edge of the sublayer. It is a self-adjusting process related to the local collapses and "bursting" phenomena discussed earlier.

For the case of $p^+ = 0.0$ and $v_o^+ = 0.0$, it is found that the critical value of $y^+$ *for this two-layer model* is $y^+ = 10.8$. But note that this is only an *effective thickness* that one obtains when using the rather artificial two-layer model. In actual fact, the viscous-dominated region is much thicker, although locally and momentarily it can be thinner. The artificiality of the thickness will be seen shortly when we compare the results of this model with experimental data.

If we introduce a pressure gradient in the direction of flow, or introduce blowing or suction at the surface, or consider a rough surface, then the critical value of $y^+$ changes. But we discuss this effect later in connection with a somewhat better sublayer model.

For the *fully turbulent region* where we intend to neglect $\nu$ relative to $\varepsilon_M$, Eq. (10-14) becomes

$$\frac{\tau_0}{\rho} = \varepsilon_M \frac{d\bar{u}}{dy}$$

Now let us introduce the Prandtl mixing-length theory, Eqs. (10-6) and (10-7). Note, then, that we are confining attention to the region for which Eq. (10-7) is valid:

$$\frac{\tau_0}{\rho} = l^2\left(\frac{d\bar{u}}{dy}\right)^2 = \kappa^2 y^2\left(\frac{d\bar{u}}{dy}\right)^2$$

Next, introduce the definitions of $u^+$ and $y^+$; after taking the root of the resulting equation, we obtain

$$\frac{du^+}{dy^+} = \frac{1}{\kappa y^+}$$

Then integrate from the outer edge of the viscous sublayer:

$$\int_{10.8}^{u^+} du^+ = \frac{1}{\kappa}\int_{10.8}^{y^+} \frac{dy^+}{y^+}$$

$$u^+ - 10.8 = \frac{1}{\kappa} \ln \frac{y^+}{10.8}$$

Setting $\kappa = 0.41$ and rearranging, we obtain the logarithmic equation that is generally called the *law of the wall:*

$$u^+ = 2.44 \ln y^+ + 5.0 \qquad (10\text{-}16)$$

A comparison with experiment is shown on Fig. 10-3. Data from three $x$ stations along a surface are plotted, along with Eq. (10-16) and Eq. (10-15). (Also shown is another model to be discussed later.) Note that the data for the three profiles depart in the outer part of the boundary layer, but they collapse together in the inner region and are well represented by Eq. (10-16) down to about $y^+ = 40$, where the effects of the sublayer begin to be seen. However, only very close to the wall do the data approach Eq. (10-15), and the artificiality represented in the two-layer model is apparent. It is of interest to note that if Eq. (10-6) is used now to determine the eddy diffusivity, we obtain $\varepsilon_M/\nu = \kappa y^+$. This is valid, however, only where there is no pressure gradient or transpiration.

In the outer part of the boundary layer, the departure of the three profiles from one another, and from Eq. (10-16), is the result of both Eqs. (10-7) and (10-13) no longer being valid, facts that were, of course, anticipated. As we go to higher and higher Reynolds numbers, the outer edge of the boundary layer goes to higher and higher values of $y^+$, and the range of $y^+$ for which Eq. (10-16) is applicable increases. At the outer edge there is still another interesting feature. For the case of no pressure gradient and no blowing or suction, the value of $u^+$ at the outer edge is always approximately 2.3 above Eq. (10-16), a fact that is observed experimentally and is also predictable if $l$ in the outer region is evaluated from Eq. (10-8) and the full partial differential equation, (10-3), is solved. The outer region in which there is a departure from the logarithmic law is frequently called the *wake region.*



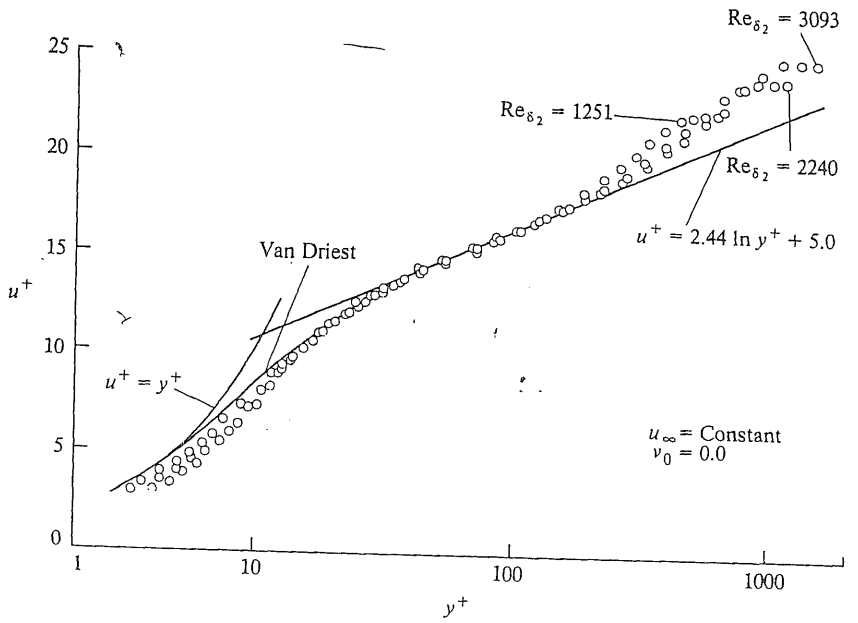


**Figure 10-3** Turbulent boundary-layer profiles in wall coordinates (*data of Anderson et al.*[13]).

Although a logarithmic form of the law of the wall generally fits the data better, a *power-law* form is sometimes more convenient. A *power law* that fits the logarithmic form fairly well out to at least $y^+ = 1500$ is

$$u^+ = 8.75y^{+1/7} \qquad (10\text{-}17)$$

Actually when the *wake region* is taken into account, Eq. (10-17) fits the true velocity profile at the outer edge a little better than the logarithmic law. Note that this equation does not fit the viscous sublayer at all; it is only an approximation for the logarithmic part. [At higher Reynolds numbers the coefficient and exponent of Eq. (10-17) must be modified in order to accurately fit Eq. (10-16).]

## AN APPROXIMATE SOLUTION TO THE MOMENTUM BOUNDARY LAYER

Equation (10-17), together with the *momentum integral equation,* can be used to obtain a relatively simple algebraic solution for the friction coefficient for a simple turbulent boundary layer. Since Eq. (10-17) was developed for the case of constant free-stream velocity, i.e., no pressure gradient, this result is likewise so restricted. However, it turns out to be quite a good approximation for rather strongly accelerated flows and a fair approximation for very mild decelerations. It is not at all useful when there is blowing or suction.

First we make the assumption that Eq. (10-17) is valid over the entire boundary layer. Let the total boundary-layer thickness be designated as $\delta$, the location at which the velocity is $u_\infty$. Then

$$\frac{u_\infty}{\sqrt{\tau_0/\rho}} = 8.75\left(\frac{\delta\sqrt{\tau_0/\rho}}{\nu}\right)^{1/7}$$

Solving for $\tau_0$,

$$\tau_0 = 0.0225\rho u_\infty^2\left(\frac{\delta u_\infty}{\nu}\right)^{-1/4} \tag{10-18}$$

Next, $\delta_1$ and $\delta_2$, the displacement and momentum thicknesses, respectively, can be evaluated by substituting Eq. (10-17) into Eqs. (5-5) and (5-6), with the results

$$\frac{\delta_1}{\delta} = 0.125 \qquad \frac{\delta_2}{\delta} = 0.097$$

From these we get the following ratio, which is used later:

$$\frac{\delta_1}{\delta_2} = 1.29 = H$$

Now Eq. (10-18) can be expressed in terms of the momentum thickness:

$$\tau_0 = 0.0125\rho u_\infty^2\left(\frac{\delta_2 u_\infty}{\nu}\right)^{-1/4} \tag{10-19}$$

Note that Eq. (10-19) provides an expression for the friction coefficient in terms of a Reynolds number based on local momentum thickness, i.e.,

$$\frac{c_f}{2} = 0.0125\ \mathrm{Re}_{\delta_2}^{-1/4} \tag{10-20}$$

Next we would like to develop a way to evaluate $\delta_2$ as a function of $x$ along the surface, and here we can use the *momentum integral equation.* Equation (5-7) for the case of $v_0 = 0.0$ and constant density becomes

$$\frac{\tau_0}{\rho u_\infty^2} = \frac{d\delta_2}{dx} + \delta_2\left[\left(2 + \frac{\delta_1}{\delta_2}\right)\left(\frac{1}{u_\infty}\right)\frac{du_\infty}{dx} + \frac{1}{R}\frac{dR}{dx}\right]$$



Substituting (10-19) for the shear stress, and using 1.29 for the shape factor $H$, yield

$$0.0125\left(\frac{u_\infty \delta_2}{\nu}\right)^{-1/4} = \frac{d\delta_2}{dx} + 3.29\left(\frac{\delta_2}{u_\infty}\right)\frac{du_\infty}{dx} + \frac{\delta_2}{R}\frac{dR}{dx}$$

This can be rearranged to

$$d(\delta_2^{5/4} R^{5/4} u_\infty^{4.11}) = 0.0156 R^{5/4} u_\infty^{3.86} \nu^{1/4}\, dx$$

Integrating with the initial condition that at $x = 0$ at least $\delta_2$, $R$, or $u_\infty$ will be zero, and solving for $\delta_2$, we get

$$\delta_2 = \frac{0.036\nu^{0.2}}{R u_\infty^{3.29}}\left(\int_0^x R^{5/4} u_\infty^{3.86}\, dx\right)^{0.8} \tag{10-21}$$

Like its laminar-flow counterpart, Eq. (7-44), this expression then involves a simple procedure that depends on a given variation of $u_\infty$ and $R$ with $x$. With $\delta_2$ established as a function of $x$, the shear stress, or the friction coefficient, is then determined from Eq. (10-19).

This equation implies that the turbulent boundary layer originates at $x = 0$, without a preceding laminar boundary-layer and a transition region. In this case, and in Eqs. (10-22) to (10-24) to follow, the point $x = 0$ is a fictitious *virtual origin* of the turbulent boundary, the point where the turbulent boundary layer *would have* originated were it not preceded by a laminar boundary layer, provided that the same turbulent transport mechanisms were applicable to zero Reynolds number.

Note that if a laminar boundary layer precedes the turbulent boundary layer, the solution to the laminar boundary layer provides the lower limit on $\delta_2$ and $x$ at the transition "point."

Let us now reduce Eq. (10-21) to the simple case of constant $u_\infty$ and constant (or very large) $R$:

$$\delta_2 = \frac{0.036\nu^{0.2}}{u_\infty^{3.29}}(u_\infty^{3.86} x)^{0.8}$$

or

$$\frac{\delta_2}{x} = \frac{0.036\nu^{0.2}}{u_\infty^{0.2} x^{0.2}} = 0.036\ \mathrm{Re}_x^{-0.2} \tag{10-22}$$

This result can now be substituted into Eq. (10-19), and after introduction of the definition of the local friction coefficient, we obtain

$$\frac{c_f}{2} = 0.0287\ \mathrm{Re}_x^{-0.2} \tag{10-23}$$

Equation (10-23) is in quite good agreement with experiments for Reynolds numbers up to several million, but becomes increasingly lower than the experimental values for higher Reynolds numbers. Probably the

definitive experimental work is that of Schultz-Grunow[14] for which he developed the empirical equation

$$\frac{c_f}{2} = 0.185(\log_{10} \mathrm{Re}_x)^{-2.584} \tag{10-24}$$

Equation (10-24) is valid for much higher Reynolds numbers than Eq. (10-23).

## EQUILIBRIUM TURBULENT BOUNDARY LAYERS

In the study of *laminar* boundary layers we found that significant simplifications occurred when attention was confined to certain classes of flows, in particular to those classes of flows which led to *similarity solutions* and geometrically similar velocity profiles.

In the study of *turbulent boundary layers* it would be convenient to be able to define some kind of similarity that would lead to a classifiable group of flows. The problem is not quite so straightforward as for laminar boundary layers. In our discussion of the law of the wall, we already observed a type of similarity in the *inner region* in $u^+$, $y^+$ coordinates, but in that coordinate system the *outer region* is not self-similar. We are now going to seek a family of flows having *outer-region similarity*, even if we have to sacrifice inner-region similarity in order to define such flows.

Clauser[15] proposed that turbulent boundary layers having outer-region similarity be called *equilibrium boundary layers* and that an equilibrium boundary layer be one for which the velocity profiles plotted in *velocity defect coordinates* be universal, i.e.,

$$\frac{\bar{u} - u_\infty}{u_\tau} = f\left(\frac{y}{\delta_3}\right)$$

independent of $x$ position, where

$$\delta_3 = -\int_0^\infty \frac{\bar{u} - u_\infty}{u_\tau}\, dy$$

Figure 10-4 shows a plot of three velocity profiles for a typical equilibrium boundary layer. (Actually this one is an adverse-pressure-gradient boundary layer with blowing.)

Clauser also proposed a *shape factor* that would be a constant, independent of $x$, under these conditions:

$$G = \int_0^\infty \left(\frac{\bar{u} - u_\infty}{u_\tau}\right)^2 d\left(\frac{y}{\delta_3}\right) \tag{10-25}$$

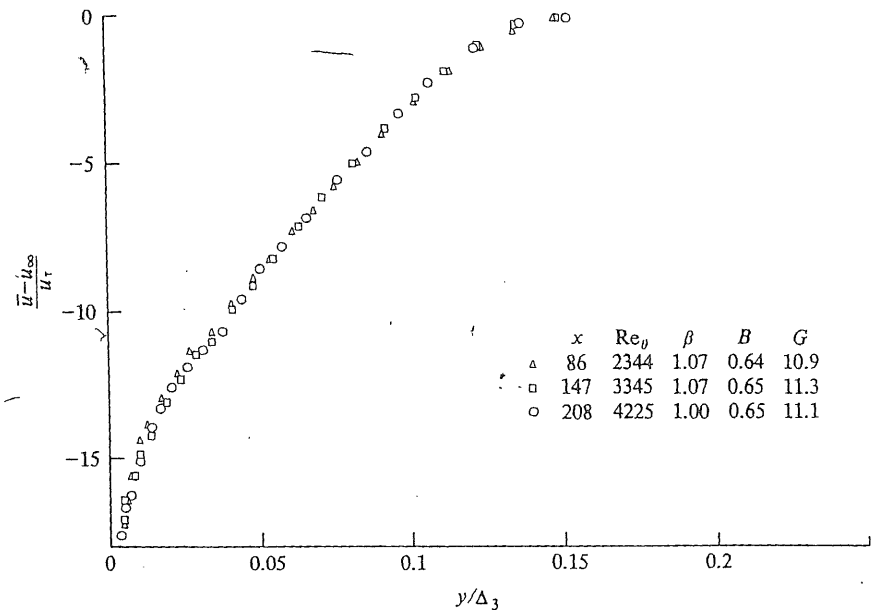


**Figure 10-4** Defect profiles for an adverse pressure gradient, transpired turbulent boundary layer (*data of Anderson et al.*[13]).

It is now instructive to examine the *momentum integral equation* which can be put in the following form (for $\rho$ constant):

$$\frac{d(u_\infty^2 \delta_2)}{dx} = \frac{\tau_0}{\rho}(1 + B_f + \beta) \tag{10-26}$$

where $B_f = \dfrac{v_0/u_\infty}{c_f/2} = \dfrac{\rho v_0 u_\infty}{\tau_0}$, a blowing or transpiration parameter

$$\beta = \frac{\delta_1}{\tau_0}\left(\frac{dP}{dx}\right), \text{ a pressure-gradient parameter}$$

$B_f$ is really the same "blowing parameter" we encountered in connection with the laminar similarity solutions, i.e., the parameter that had to be maintained constant (recall that $c_f/2$ varies as $1/\sqrt{\mathrm{Re}_x}$ for laminar boundary layers). But its *physical* interpretation can be seen in the second identity. It is the ratio of the *transpired momentum flux* to the *wall shear force*, and thus this ratio is being maintained constant when the laminar similarity solutions for blowing or suction are obtained.

$\beta$ is another force ratio, axial *pressure forces* to *wall shear force*. Note that the overall equation expresses the rate of growth of the momentum deficit of the boundary layer.

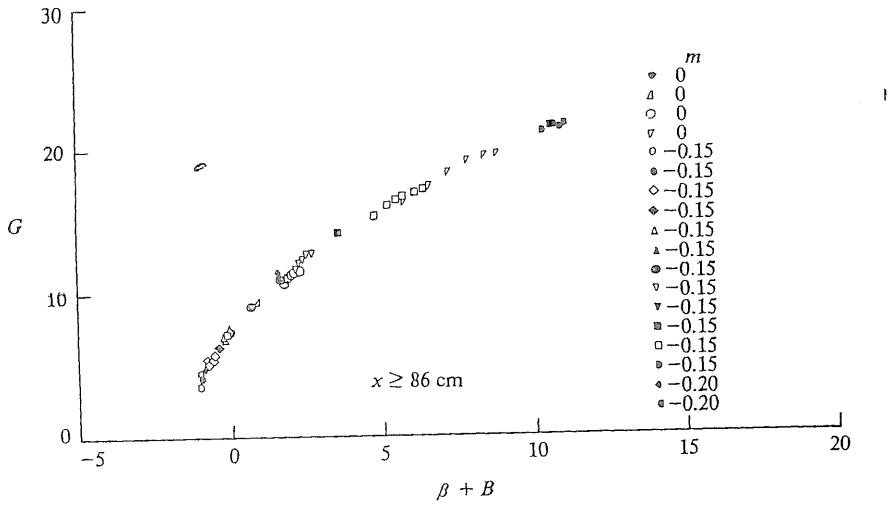


Figure 10-5 Clauser shape factor for a variety of equilibrium turbulent boundary layers (*data of Anderson et al.*[13]).

We find experimentally that if for a turbulent boundary layer we hold $B_f$ or $\beta$ or both constant, we also observe outer-region similarity and $G$ is constant. As a matter of fact, we find that $G$ is a unique function of $B_f + \beta$, as can be seen from the experimental data plotted in Fig. 10-5, data that include a variety of combinations of $B_f$ and $\beta$.

Finally a question remains as to how free-stream velocity or axial pressure gradient must vary in order to hold $\beta$ constant. For a laminar boundary layer it was found that similarity solutions were obtained if

$$u_\infty = Cx^m$$

Not too surprisingly, the same free-stream velocity variation for a turbulent boundary layer leads to constant $G$, that is, to equilibrium boundary layers having outer-region similarity.

Another rather special class of equilibrium boundary layers occurs in accelerating flows if an acceleration parameter $K$ is maintained constant along the surface:

$$K = \frac{\nu}{u_\infty^2}\frac{du_\infty}{dx} \tag{10-27}$$

By making use of this parameter, the momentum integral equation (for plane flows and constant density) may be written

$$\frac{d\,\mathrm{Re}_{\delta_2}}{u_\infty\, dx/\nu} = \frac{c_f}{2} + \frac{v_0}{u_\infty} - K(1+H)\,\mathrm{Re}_{\delta_2} \tag{10-28}$$



If $K$ and $v_0/u_\infty$ are maintained constant with respect to $x$, if $K$ is *positive*, and if the last term is larger than the second, then the boundary layer inevitably approaches an equilibrium condition for which $\mathrm{Re}_{\delta_2}$ is constant. We speak of this as an *asymptotic accelerating flow*. Actually it is a boundary layer that has both inner and outer similarity; not only is $\mathrm{Re}_{\delta_2}$ constant, but so also are $c_f/2$, $H$, $G$, and $\beta$.

Note that for $K = 0$ an asymptotic layer will be reached for negative values of $v_0/u_\infty$, that is, constant suction. This is spoken of as the *asymptotic suction layer.*

The value of $\mathrm{Re}_{\delta_2}$ at the point of equilibrium depends on $K$, large values of $K$ leading to low $\mathrm{Re}_{\delta_2}$. Note that $\mathrm{Re}_{\delta_2}$ can *decrease* in the flow direction if $K$ is large. If $K$ is sufficiently large, the equilibrium value of $\mathrm{Re}_{\delta_2}$ can be below the critical Reynolds number for transition from a laminar to a turbulent boundary layer, in which case turbulence production ceases and a laminar boundary layer reemerges. Experimentally this phenomenon, which is often called *laminarization*, occurs when $K$ exceeds about $3 \times 10^{-6}$, although "laminarlike" *heat-transfer* behavior is observed at considerably lower values of $K$ for reasons to be seen later. This phenomenon is frequently observed in highly accelerated flows in nozzles (see, for example, Back, Cuffel, and Massier[16]).

## THE TRANSPIRED TURBULENT BOUNDARY LAYER

So far we have discussed only turbulent boundary layers for which the normal component of velocity at the surface $v_0$ is zero, i.e., the case of the impermeable wall. Nonzero values of $v_0$ can occur if the wall is porous and either fluid is "blown" or injected into the boundary layer or is withdrawn or "sucked." Evaporation or condensation or mass transfer in general leads to nonzero values of $v_0$. We use the term *transpiration*, or the *transpired* boundary layer, as a general description interchangeably with blowing, suction, injection, mass transfer at the surface, etc. Reviews of the effects of transpiration on the turbulent boundary layer can be found in Kays[17] and Kays and Moffat.[18]

For laminar boundary layers it was found that *similarity solutions* exist for nonzero values of $v_0$ provided that a *blowing parameter*, essentially $B_f$, is maintained constant. We have already noted that constant $B_f$ results in an *equilibrium* turbulent boundary layer.

Transpiration alters the structure of the turbulent boundary layer rather considerably, affecting the shear-stress distribution [see Eq. (10-13)], and also strongly affecting the sublayer thickness. It is perfectly feasible to develop a two-layer model for this boundary layer, and the only new information needed is a relation between $v_0^+$ and the value of $y^+$ at the outer edge of the sublayer. The experimental evidence is that the mixing-length con-

stant $\kappa$ is unchanged and that the outer-region mixing-length constant $\lambda$ is unaffected. A transpiration law of the wall comparable to Eq. (10-16) but with an additional log-squared term is readily derivable. However, all this is much better handled in the context of a continuous sublayer model which is discussed later (although then we are restricted to machine computation rather than simple algebraic results). In the meantime, it proves useful to develop a rather simple algebraic Couette flow solution which has the happy virtue of fitting the experimental data surprisingly well.

Consider Eq. (10-3) under the conditions of no pressure gradient, and apply the Couette flow approximation.

$$v_0 \frac{d\bar{u}}{dy} - \frac{d}{dy}\left[(\nu + \varepsilon_M)\frac{d\bar{u}}{dy}\right] = 0$$

Let the boundary conditions be

$$\text{At} \quad y = 0 \qquad \bar{u} = 0, \qquad \frac{\tau_0}{\rho} = \nu\left(\frac{d\bar{u}}{dy}\right)_0$$

$$\text{At} \quad y = \delta \qquad \bar{u} = u_\infty$$

Integrating once and applying the first boundary condition,

$$v_0 \bar{u} - (\nu + \varepsilon_M)\frac{d\bar{u}}{dy} = -\frac{\tau_0}{\rho}$$

Rearranging, and integrating across the boundary layer, yield

$$\int_0^{u_\infty} \frac{d\bar{u}}{v_0 \bar{u} + \tau_0/\rho} = \int_0^\delta \frac{dy}{\nu + \varepsilon_M}$$

$$\frac{1}{v_0} \ln\left[1 + \frac{v_0 u_\infty \rho}{\tau_0}\right] = \int_0^\delta \frac{dy}{\nu + \varepsilon_M}$$

But note that

$$\frac{v_0 u_\infty \rho}{\tau_0} = B_f = \frac{v_0/u_\infty}{c_f/2}$$

Then

$$\ln(1 + B_f) = \frac{c_f}{2} B_f u_\infty \int_0^\delta \frac{dy}{\nu + \varepsilon_M}$$

$$\frac{c_f}{2} = \frac{\ln(1 + B_f)}{B_f} \frac{1}{u_\infty}\left(\int_0^\delta \frac{dy}{\nu + \varepsilon_M}\right)^{-1}$$

This equation is indeterminant for $B_f = 0$, but

$$\lim_{B_f \to 0} \frac{\ln(1 + B_f)}{B_f} = 1.0$$

So,

$$\left(\frac{\overline{c_f}}{2}\right)_0 = \frac{1}{u_\infty}\left(\int_0^\delta \frac{dy}{\nu + \varepsilon_M}\right)^{-1}$$

where subscript 0 refers to the $B_f = 0.0$ case.

Then if we make the assumption (obviously not proved) that the two integrals are independent of $B_f$, then

$$\frac{c_f/2}{(c_f/2)_0} = \frac{\ln(1 + B_f)}{B_f} \tag{10-29}$$

We find that Eq. (10-29) is an excellent representation of the available experimental evidence for the no-pressure gradient case if $(c_f/2)_0$ is evaluated at the same $x$ *Reynolds* number. Thus we can use Eq. (10-23) to obtain

$$\frac{c_f}{2} = 0.0287 \frac{\ln(1 + B_f)}{B_f} \mathrm{Re}_x^{-0.2} \tag{10-30}$$

By use of the momentum integral equation this result can also be expressed as a function of the *momentum thickness* Reynolds number:

$$\frac{c_f}{2} = 0.0125\left[\frac{\ln(1 + B_f)}{B_f}\right]^{1.25} (1 + B_f)^{0.25} \mathrm{Re}_{\delta_2}^{-0.25} \tag{10-31}$$

Experimental data indicate that the function $(c_f/2)/(c_f/2)_0$ implied by Eq. (10-31) applies equally well in pressure gradients if the comparison is made at the same value of $\mathrm{Re}_{\delta_2}$. Furthermore, although the experiments for which these relations have been established were generally carried out at constant $B_f$ (i.e., equilibrium boundary layers), it is also found that they hold quite well if $B_f$ varies moderately along the surface, as, for example, when $v_0/u_\infty$ is held constant rather than $B_f$. This is simply because the inner viscous region of the turbulent boundary layer comes into "equilibrium" very quickly.

Because we have specified a constant-density fluid throughout this discussion, density canceled out of the defining equation for $B_f$, leaving a velocity ratio $v_0/u_\infty$. If the numerator and denominator are multiplied by $\rho$, this becomes a mass flux ratio, and it is really mass flux rather than velocity that is responsible for the phenomena observed. Since many applications, and especially gas applications, involve significant density differences across the boundary layer, a preferred definition for $B_f$ is

$$B_f = \frac{\dot{m}''/G_\infty}{c_f/2}$$

where $\dot{m}''$ is the mass flux at the wall surface, and $G_\infty$ is the free-stream mass flux, that is, $G_\infty = u_\infty \rho_\infty$.

Another "blowing parameter" frequently used is

$$b_f = \frac{\dot{m}''/G_\infty}{(c_f/2)_0}$$

From Eq. (10-29) we then find that $b_f = \ln(1 + B_f)$, and then

$$\frac{c_f/2}{(c_f/2)_0} = \frac{b_f}{e^{b_f} - 1} \tag{10-32}$$

It is frequently more convenient to use $b_f$ than $B_f$ in the evaluation of $c_f$ because of the implicit nature of such an equation as (10-30).

Two limits to the transpired boundary layer should be pointed out. One, the *asymptotic suction layer*, was described in the discussion of equilibrium boundary layers. From Eq. (10-28), for $K = 0.0$, a constant negative value of $v_0/u_\infty$ (or $\dot{m}''/G_\infty$) leads to constant $\mathrm{Re}_{\delta_2}$, and then

$$\frac{c_f}{2} = -\frac{\dot{m}''}{G_\infty}$$

which is a *lower* limit on the friction coefficient.

The second limit occurs at large values of blowing when the friction coefficient tends to zero and the boundary layer is literally blown off the surface, an occurrence similar to the *separation* of a boundary layer in an adverse pressure gradient. Two commonly used rules of thumb for "blow-off" are $\dot{m}''/G_\infty = 0.01$ and $b_f = 4.0$.

## A CONTINUOUS LAW OF THE WALL: THE VAN DRIEST MODEL

It is quite possible to improve upon the two-layer model of the turbulent boundary layer in a number of ways, but any model that involves a totally viscous sublayer ($\varepsilon_M = 0.0$), while perhaps perfectly satisfactory for solution of the momentum equation, can lead to substantial underprediction of heat transfer, especially at high Prandtl numbers. The reason is that a very small eddy diffusivity in the region $y^+ < 5.0$ can contribute greatly to the heat-transfer rate while having a negligible effect on momentum transfer.

The concept of a sublayer in which relatively large elements of fluid lift off the surface, to be replaced immediately by other fluid from the fully turbulent region, the "bursting" phenomenon discussed earlier, demands a sublayer model for which the eddy diffusivity retains a finite magnitude throughout the sublayer and goes to zero only at the wall itself. The idea that $\varepsilon_M$ is nonzero, though very small, very near the wall does not mean we are talking about *small turbulent eddies*. $\varepsilon_M$ is a statistical quantity averaged over time and space, and very small $\varepsilon_M$ in the sublayer merely implies a relatively infrequent event.



The Van Driest hypothesis[19] is a sublayer scheme that provides for an eddy diffusivity which is only 0.0 at $y = 0.0$ and which also has the virtue that it allows a continuous calculation through the sublayer and into the fully turbulent region with no discontinuities. At the same time it does a reasonable job of predicting the various flow parameters throughout the entire sublayer region. Other schemes will do much the same thing, so the particular function used in the Van Driest hypothesis should not be regarded as having any theoretical basis.

With this scheme we use the Prandtl mixing length all the way to the wall instead of truncating it to zero at an assumed outer edge of the sublayer, but we simulate the sublayer by introducing a damping function into the mixing-length equation, (10-7). An exponential function is convenient, so Van Driest proposed that

$$l = \kappa y\left(1 - \frac{1}{e^{y/A}}\right)$$

The constant $A$ is an empirically determined effective sublayer thickness, but since it is a dimensional quantity, and we have previously argued that the sublayer thickness should be expressed as a local thickness Reynolds number, we should express the exponent as $y^+/A^+$. Then

$$l = \kappa y\left(1 - \frac{1}{e^{y^+/A^+}}\right) \tag{10-33}$$

We now propose to evaluate the total shear stress using Eqs. (10-6) and (10-9) throughout the entire boundary layer, without neglecting either $\varepsilon_M$ or $\nu$ anywhere. If we confine attention to the region relatively near the wall, we can still make the Couette flow assumption, but we *are* forced to make computer calculations and simple algebraic solutions are no longer feasible.

There remains the problem of determining $A^+$. This is done by simply assuming various values of $A^+$ and carrying out calculations until the calculated values of $u^+$ outside the sublayer correspond to experiment, or for the most simple case to the "law of the wall," Eq. (10-16). The results of such calculations for $A^+ = 25.0$ are shown in Fig. 10-3.

$A^+ = 25.0$ is determined for a boundary layer with no pressure gradient or transpiration; it is found that both pressure gradient and transpiration (as well as surface roughness and perhaps other effects) have a pronounced effect on $A^+$. Since $A^+$ is simply an effective sublayer thickness, these other parameters apparently influence the sublayer thickness. A favorable pressure gradient (accelerating flow) induces a thicker sublayer; an adverse pressure gradient has the opposite effect. Blowing decreases $A^+$ while suction increases $A^+$. Roughness, discussed later, decreases $A^+$. These results are not surprising when one contemplates the probable influence of these effects on the stability of the viscous sublayer.

An empirical equation for $A^+$ as a function of the pressure gradient parameter $p^+$ and the transpiration parameter $v_0^+$, based on the Stanford experimental data,[18] is

$$A^+ = \frac{25.0}{a\{v_0^+ + b[p^+/(1 + cv_0^+)]\} + 1.0} \tag{10-34}$$

where $a = 7.1 \quad b = 4.25 \quad c = 10.0$
If $p^+ > 0.0 \quad b = 2.9, c = 0.0$
If $v_0^+ < 0.0 \quad a = 9.0$

A plausible theoretical basis for this result (but not the form of this equation) can be developed if we hypothesize that the sublayer adjusts itself such that a "Reynolds number of turbulence" always has the same critical value at the outer edge. The Reynolds number of turbulence is defined:

$$\mathrm{Re}_t = \frac{l_t\sqrt{\overline{u'v'}}}{\nu} = \frac{l_t\sqrt{\tau_t/\rho}}{\nu} \tag{10-35}$$

where $l_t$ is a "turbulence-length scale" and $\tau_t$ is the turbulent shear stress. Now examine the definition of $y^+$, and then note that just *outside* the sublayer the mixing length $l = \kappa y$ and $\tau \approx \tau_t$. Then

$$y^+ = \frac{y\sqrt{\tau_0/\rho}}{\nu} = \frac{1}{\kappa}\frac{l\sqrt{\tau_t/\rho}}{\nu}\sqrt{\frac{\tau_0}{\tau}}$$

It seems plausible to identify the turbulence-length scale with the *mixing length*, in which case we can write

$$\mathrm{Re}_t = ky^+\sqrt{\frac{\tau}{\tau_0}}$$

It has been found from experimental data[13] that if the edge of the sublayer is defined as $y^+_{\text{edge}} = 3A^+$, then $\mathrm{Re}_t$ has a value of about 31 regardless of $v_0^+$ and/or $p^+$. Thus

$$31 = 0.41(3A^+)\sqrt{(\tau/\tau_0)_{y^+=3A^+}}$$

$$A^+ = \frac{25.0}{\sqrt{(\tau/\tau_0)_{y^+=3A^+}}} \tag{10-36}$$

A series of "computer experiments" can then be carried out for various values of $v_0^+$ and $p^+$, and it is found that the results, $A^+(v_0^+, p^+)$, are close to those given by Eq. (10-34). Furthermore, Eq. (10-13), together with (10-36), immediately shows qualitatively the influence of pressure gradient and transpiration.

## SUMMARY OF A COMPLETE MIXING-LENGTH THEORY

In the preceding sections we have alternately discussed the elements of a complete mixing-length theory and various approximate procedures that lead to simple algebraic solutions. For the sake of clarity it is now worthwhile to briefly summarize the complete mixing-length theory which does, however, require a finite-difference procedure and a digital computer for implementation.

The momentum boundary-layer differential equation to be solved, together with the appropriate version of the continuity equation and any desired boundary and initial conditions, is Eq. (10-3).

The eddy diffusivity $\varepsilon_M$ is then replaced by Eq. (10-6). In the outer part of the boundary layer, the mixing-length $l$ is evaluated from Eq. (10-8), while in the inner part $l$ is evaluated from Eq. (10-33). The intersection of the outer and inner parts is determined by equating Eqs. (10-7) and (10-8).

An alternative and frequently used method for calculating the outer part of the boundary layer is to assume that $\varepsilon_M$ is constant over that region (which is approximately true). In the outer region $\varepsilon_M$ is then found to be a simple function of a boundary-layer thickness Reynolds number, either $\mathrm{Re}_{\delta_1}$ or $\mathrm{Re}_{\delta_2}$; that is, the following empirical equation can be used once the constants are established from experiments:

$$\frac{\varepsilon_M}{\nu} = a\,\mathrm{Re}_{\delta_1}^b \tag{10-37}$$

The effective sublayer thickness $A^+$ can be evaluated from Eq. (10-34), although it is also possible to make use of Eq. (10-36).

One difficulty that arises in using Eq. (10-34) is that the sublayer thickness does not instantaneously change when $p^+$ and/or $v_0^+$ are abruptly changed. A new state of sublayer equilibrium may not obtain for some distance along the surface. The following rate equation provides a convenient and reasonably practicable way to handle this problem:

$$\frac{dA^+}{dx^+} = \frac{A^+_{\text{eq}} - A^+}{C} \tag{10-38}$$

where $A^+_{\text{eq}}$ is the value determined from Eq. (10-34), $x^+ = x\sqrt{\tau_0/\rho}/\nu$, and $C$ is an empirical constant. A value of $C = 4000$ has been frequently used.

## THE EFFECTS OF SURFACE ROUGHNESS

In all the preceding discussion of the turbulent boundary layer, it has been assumed that the surface is "aerodynamically smooth," without defining what that term implies. At this point it is appropriate to discuss a rational

definition of roughness, so as to establish the limits of the theory already presented, and then to describe some of the effects of roughness.

Surface roughness can take on many shapes. The name of Nikuradse[20] is indelibly associated with the rational analysis of rough surfaces as a result of his experiments with turbulent flow in pipes that were artificially roughened with uniform grains of sand. Schlichting[21] introduced the concept of *equivalent sand-grain roughness* as a means of characterizing other types of roughness elements by referring to the equivalent net effect produced by Nikuradse's experiments. We use the symbol $k_s$, a length dimension, to describe roughness element size, $k_s$ being actually the size of the sieve used by Nikuradse to sift the sand.

The effect of roughness on a turbulent boundary layer is primarily right at the wall, and thus a nondimensional expression of roughness size is logically based on the shear velocity $u_\tau$. This leads to a *roughness Reynolds number* $\mathrm{Re}_k$ as a nondimensional measure of surface roughness:

$$\mathrm{Re}_k = \frac{u_\tau k_s}{\nu}$$

Three regimes of roughness can be identified from the experimental data in terms of values of $\mathrm{Re}_k$. For $\mathrm{Re}_k < 5.0$ the surface behaves as perfectly smooth (aerodynamically smooth). For $5.0 < \mathrm{Re}_k < 70.0$ there is an increasing effect of roughness but some of the smooth-surface characteristics persist, and this is called the range of *transitional* roughness. The range $\mathrm{Re}_k > 70.0$ is the regime of the *fully rough* surface. A basic characteristic of the fully rough surface is that the friction coefficient $c_f$ becomes independent of Reynolds number, which means essentially that *viscosity* is no longer a significant variable.

A mixing-length model for the *fully rough* region can be readily developed. The first effect of roughness is to destabilize the viscous sublayer, which results in an effectively thinner sublayer. At about $\mathrm{Re}_k = 70$ the sublayer disappears entirely, which accounts for the fact that viscosity is no longer a significant variable. But this also means that the shear stress must be transmitted to the wall by some different mechanism. This different mechanism is quite obviously pressure drag directly on the roughness elements, i.e., a result of impact or dynamic pressure on the upstream side of each element. If the Prandtl mixing-length scheme is used, it is apparent that Eq. (10-7) is no longer valid at the wall surface because $l$, and thus $\varepsilon_M$, cannot go to zero at the wall. The eddy diffusivity and mixing length must obviously be finite at $y = 0$ for a fully rough surface. This can be readily modeled by a near-wall mixing-length equation:

$$l = \kappa(y + \delta y_0) \tag{10-39}$$

where $\delta y_0$ might be expected to be proportional to $k_s$ (actually $\delta y_0$ turns out to be considerably smaller than $k_s$). In using the wall coordinate scheme, the



nondimensional form of $\delta y_0$ is $(\delta y_0)^+$, that is,

$$(\delta y_0)^+ = \frac{\delta y_0 u_\tau}{\nu} \tag{10-40}$$

Experimentally it is found that, approximately,

$$(\delta y_0)^+ = 0.031\ \mathrm{Re}_k \tag{10-41}$$

To develop a law of the wall for the fully rough region, we go back to the development leading to Eq. (10-16) and simply replace $l = \kappa y$ with Eq. (10-39). This then leads to

$$\frac{du^+}{dy^+} = \frac{1}{\kappa[y^+ + (\delta y_0)^+]}$$

Since there is no sublayer in the fully rough region, the lower limit of integration of this differential equation is at $y^+ = 0$.

$$\int_0^{u^+} du^+ = \frac{1}{\kappa}\int_0^{y^+} \frac{dy^+}{y^+ + (\delta y_0)^+}$$

$$u^+ = \frac{1}{\kappa} \ln \left[\frac{y^+}{(\delta y_0)^+} + 1\right] \tag{10-42}$$

Then substitute (10-41):

$$u^+ = \frac{1}{\kappa} \ln \left(\frac{32.6y^+}{\mathrm{Re}_k} + 1\right) \tag{10-43}$$

For $y^+ \geq \mathrm{Re}_k$ the last term in the parentheses can be neglected and a simpler form results:

$$u^+ = \frac{1}{\kappa} \ln y^+ + \frac{1}{\kappa} \ln \frac{32.6}{\mathrm{Re}_k} \tag{10-44}$$

Equation (10-44) fits the available experimental data in the fully rough region for no pressure gradient and no transpiration quite well, using $\kappa = 0.41$.[22]

An approximate expression for the friction coefficient under the same conditions can be readily developed from Eq. (10-44). Recall it was noted in connection with Eq. (10-16) that at the outer edge of the boundary layer $u^+$ is always greater than the law of the wall by an additive 2.3. Assuming that the same wake effect obtains for a rough-surface boundary layer, Eq. (10-44) can be modified to yield the value of $u^+$ at the outer edge of the boundary layer

$$u_\infty^+ = \frac{1}{\kappa} \ln \frac{\delta u_\tau}{\nu} + \frac{1}{\kappa} \ln \frac{32.6}{\mathrm{Re}_k} + 2.3$$

Then, noting that

$$u_\infty^+ = \frac{u_\infty}{u_\tau} = \frac{1}{\sqrt{c_f/2}}$$

we obtain

$$\frac{1}{\sqrt{c_f/2}} = \frac{1}{\kappa} \ln \frac{84\delta}{k_s}$$

Then, if $\delta_2/\delta = 0.097$ still applies,

$$\frac{c_f}{2} = \frac{0.168}{[\ln (864\delta_2/k_s)]^2} \tag{10-45}$$

Note that $c_f$ depends only on boundary-layer thickness and the roughness size and is independent of viscosity and velocity. This equation fits the experimental data of Pimenta, Moffat, and Kays[22] quite well. To express $c_f/2$ as a function of distance $x$ along the surface, the momentum integral equation can be used.

If free-stream velocity varies along the surface, the problem is best solved using the complete boundary-layer equations and finite-difference methods and employing a computer. The same mixing-length theory can be used. In the transitional roughness region ($5 < \mathrm{Re}_k < 70$) the effect of a thinner sublayer can be modeled by using a function $A^+(\mathrm{Re}_k)$ that decreases continuously from the smooth-surface value at $\mathrm{Re}_k = 5$ to zero at $\mathrm{Re}_k = 70$. For $\mathrm{Re}_k > 70$, $A^+ = 0.0$; and the only other modification that needs to be made is to employ Eq. (10-39) for the mixing length. However, for this type of calculation $(\delta y_0)^+$ is better approximated by

$$(\delta y_0)^+ = 0.031(\mathrm{Re}_k - 43) \tag{10-46}$$

rather than by Eq. (10-41).

In the outer part of the boundary layer, Eq. (10-8) can again be used as for a smooth surface.

## THE EFFECTS OF AXIAL PRESSURE GRADIENT

The influence of either a positive or negative pressure gradient in the direction of flow is included in the empirical correlation for $A^+$, Eq. (10-34), and the mixing-length theory that is described will predict the effects of pressure gradient quite adequately, except for the region very near separation. Boundary-layer separation, or stall, occurs when a strong adverse (positive) pressure gradient causes a reversal of the velocity profile near the wall and the wall shear stress tends to zero. The mechanics of the separation or stall process are complex and beyond the scope of this book. The reader should be cautioned, however, that when attempting to predict boundary-layer behavior with an adverse pressure gradient (i.e., positive pressure gradient and a decelerating free-stream velocity), the behavior of the friction coefficient should be observed; and a rapidly decreasing tendency should be a signal of possible stall and an indication that the mixing-length theory is inadequate to predict subsequent boundary-layer behavior.

In the discussion of equilibrium boundary layers a pressure gradient parameter $\beta$ is introduced. A constant positive value of $\beta$ leads to an equilibrium adverse pressure gradient boundary layer that will not tend toward stall.

The effect of an adverse pressure gradient is to decrease $c_f$; and for equilibrium boundary layers, the reduction of $c_f$ can be rather simply correlated with $\beta$. (Note the similarity to the influence of the blowing parameter $B_f$.) The following empirical relation has been found to reasonably correlate the results of equilibrium adverse pressure gradient (constant positive values of $\beta$) computer calculations using the mixing-length theory of the preceding sections. As such, it can then be applied as a correction to Eq. (10-20), or to Eq. (10-31).

$$\frac{c_f}{c_{f,\beta=0}} = \frac{1}{1 + \beta/5} \tag{10-47}$$

A favorable pressure gradient leads to negative values of $\beta$ and an increase of $c_f$ relative to Eq. (10-20). However, $\beta$ tends to have a very small magnitude for most practicable accelerating flows. As discussed previously, strong acceleration leads to asymptotic boundary layers and laminarization, both of which phenomena can be adequately predicted without this correction, i.e., using Eqs. (10-21) and (10-20).

We now have available most of the necessary tools to construct a complete integral equation theory for the momentum equation for both pressure gradient and transpiration, based on an assumption of local equilibrium. All that is missing is the shape factor $H$, which appears in the momentum integral equation. A simple relation between $H$ and the Clauser shape factor $G$ can be developed from the defining equations for these parameters.

$$H = \frac{1}{1 - G(c_f/2)^{1/2}} \tag{10-48}$$

Experimental data on $G$ as a function of $(B_f + \beta)$ are available in Fig. 10-5.

However, one now has to consider carefully whether the implied integral procedure, which is fairly complex and requires numerical implementation, holds any advantage over a complete numerical solution of the momentum differential equation.

## HIGHER-ORDER MODELS OF TURBULENCE

The mixing-length theory described in this chapter has proved quite adequate for plane turbulent boundary layers under a reasonably wide variety of conditions, and thus provides a very versatile engineering tool. However, it is not really adequate when there are very large departures from equilibrium; when there is large free-stream turbulence and large surface curvature; and where there are three-dimensional effects. The mixing-length theory tends to fail near separation or for flow conditions that have inflected velocity profiles. For the case of general three-dimensional flows where the boundary-layer approximations do not apply, the mixing-length theory becomes totally inadequate.

These limitations have given rise to the development of a succession of what might be termed *higher-order* theories of turbulent transport that involve the necessity of solving one or more additional partial differential equations. Some degree of success has been obtained, but at this writing there is no clear consensus as to an ultimate theory, and the use of high-order theories as common engineering tools is still apparently some time away. Only a very brief description of some of these theories is given here.

A popular starting point for high-order models is the *turbulent kinetic energy equation.* This equation can be derived by manipulation of the Navier-Stokes equations, and it expresses the production, convection, diffusion, and dissipation of the kinetic energy associated with the turbulent fluctuating quantities $u'$, $v'$, etc. A partial differential equation similar in form to the thermal energy equation is obtained. Its solution provides local values of the turbulent energy, and then the eddy diffusivity is determined from an assumed relationship between the eddy diffusivity and the turbulent energy. A *turbulence-length scale* is also needed in this relation; in the so-called one-equation models the length scale is provided through simple empirical relations similar to mixing-length relations.

In the *two-equation models* another partial differential equation is solved to provide local values for the length scale. Considerable success has been obtained by using an equation derivable by manipulation of the Navier-Stokes equations, this time an equation for the isotropic dissipation, a term that appears in the turbulent kinetic energy equation. The two-equation models appear to be the very least that is needed to handle three-dimensional flows.

The next level of models, sometimes termed *stress-equation models,* involves solutions of partial differential equations for all the components of the turbulent stress tensor. A still higher level involves computations of the three-dimensional time-dependent large-eddy structure together with a lower-level model for the small-scale turbulence.



Detailed descriptions of some boundary-layer computation schemes can be found in Refs. 23 and 24. Summaries of computational schemes and turbulence models, together with extensive lists of references, are given by Reynolds[25] and Reynolds and Cebeci.[26]

## PROBLEMS

**10-1** Using the Van Driest equation for the mixing length in the sublayer, determine $u^+$ as a function of $y^+$ for $p^+ = 0$ and $v_0^+ = 0$ by numerical integration of the momentum equation in the region where the Couette flow approximation is valid, for $A^+ = 22$, 25, 27, and compare with the experimental data in Fig. 10-3. (It is presumed that a programmable computer is used for this problem.)

**10-2** Develop a law of the wall for a transpired turbulent boundary layer (that is, $v_0 \neq 0$) based on the Prandtl mixing-length theory and a two-layer model of the Couette flow region near the wall. Note that you need to develop a new relation for both the viscous sublayer and the fully turbulent region, and the apparent thickness of the sublayer will be a constant to be determined from experiments.

The following are two sets of experimental points for turbulent velocity profiles for $p^+ = 0.0$ but $v_0^+ \neq 0$.

| $v_0^+ = 0.1773$ | | $v_0^+ = -0.065$ | |
|---|---|---|---|
| $y^+$ | $u^+$ | $y^+$ | $u^+$ |
| 30.6 | 16.84 | 35.6 | 12.33 |
| 50.3 | 19.37 | 48.7 | 13.02 |
| 99.6 | 23.41 | 81.7 | 13.59 |
| 148.9 | 25.72 | 150.8 | 14.24 |
| 247.6 | 29.99 | 249.6 | 14.80 |
| 362.6 | 34.11 | 364.8 | 15.34 |
| 510.6 | 39.36 | 496.5 | 15.87 |
| 724.3 | 45.13 | 628.2 | 16.20 |
| 921.5 | 47.29 | 792.8 | 16.31 |
| 1053.0 | 47.32 | 990.4 | 16.31 |

Plot these profiles on semilog paper and superimpose the equation you have derived for the fully turbulent region, determining the apparent sublayer thickness from the best fit to the data. Note that there is a "wake" or outer region for which your analysis does not apply. Finally, plot apparent sublayer thickness $y^+_{crit}$ as a function of $v_0^+$ and discuss the significance of the results.

**10-3** Repeat Prob. 10-2 using the Van Driest equation for the sublayer mixing length and numerical integration of the momentum equation. Determine the values of $A^+$ which best fit the experimental data, and plot these as a function of $v_0^+$. (It is presumed that a programmable computer is used for this problem.)